WELDING RESEARCH

SUPPLEMENT TO THE *WELDING JOURNAL*, 2024
Sponsored by the American Welding Society

Comments on the Numerical Models for Correlating Weld Metal Composition to Microstructure and Properties

Microalloying elements effects need to be considered in consumable design rules

BY G. M. EVANS, M. A. QUINTANA, AND S. S. BABU

Introduction

There has been a steady rise in the use of computational tools to model or describe weld microstructure and properties from data sets containing a wide range of inputs and outputs measured by experiments. The tools range in sophistication from simple two-factor correlations in spreadsheets to artificial neural networks. The effectiveness of resulting models to predict outcomes often depends less on the sophistication of the tools and more on

1. The physical realities of the materials under investigation, and

2. A willingness to critically assess the limitations of the methodology in use.

Recent papers (Refs. 1–3) published in the *Welding Journal* are worth a second look in this context. In these papers, authors analyzed a large body of historical data by Evans (Ref. 4) for low hydrogen shielded metal arc low alloy steel weld metal, released in 2015, to develop design rules for welding electrodes that would consistently exceed specification requirements. Authors (Refs. 1, 2) first apply a series of spreadsheet filters to reduce the volume of data under consideration at any one time to a manageable level and supplement from their own experience as well as other publicly available internet tools (Ref. 5) that are based on published artificial neural networks (Ref. 6) and dilatometric data (Ref. 7). A series of statistical and regression correlations were used to generalize the effects of Ti-B-Al-O-N on microstructure development and weld properties. This simple spreadsheet-based approach is appealing to engineers facing large data sets without access to more sophisticated computational tools. However, there is a risk that oversimplification may lead to erroneous predictions and conformation bias even with an understanding of the role of microalloying additions on the weld microstructure and resulting properties.

https://doi.org/10.29391/2024.103.012

Methodology

The Ti-B-Al-O-N series from Evans's historical data included a total of 24 multi-run combinations, covering a wide range of microalloying variations at parts per million levels (Ti 1 to 540; B: 1 to 195; Al: 1 to 580; N: 41 to 249; and O: 281 to 503). All other alloying elements (e.g., C, Si, and Mn) were held as consistent as possible. The subset selection used by Authors (Refs. 1–3) started at 13 of the original 24 data sets (see Table 1). The same microalloy ranges are represented but with fewer combinations. This work reconsiders several topics in the context of all 24 data sets to illustrate the potential risk of oversimplification. These include (a) the correlation between microalloying and toughness; (b) the correlation between carbon equivalence and properties; (c) the role of transformation starting temperatures and (d) overreliance on neural network.

Results and Discussion

Toughness and microalloying: The subset of 13 data sets used by the authors in references 1 and 2 was the result of multiple reduction cycles. To achieve favorable numerical optimizations, authors first limited carbon to < 0.1% and CEN to < 0.3%. Further down selection of "specific alloy additions" for consideration of transformation start (T_s) and finish temperatures resulted in the final sub-set of 13.

This significantly reduced the amount of data accessible for the assessment of weld toughness, which focused on 28J transition temperatures and "independent" validation using Japanese Welding Engineering Society (JWES) neural net predictions. However, if the Charpy-V absorbed energy versus temperature curves for the full series of 24 (Fig. 1A) are considered, a lateral shift of 100°C is apparent close to the ductile to brittle transition region that is due to minor changes in microalloying content. For example, comparing the weld X (included in the sub-set) and T (omitted from

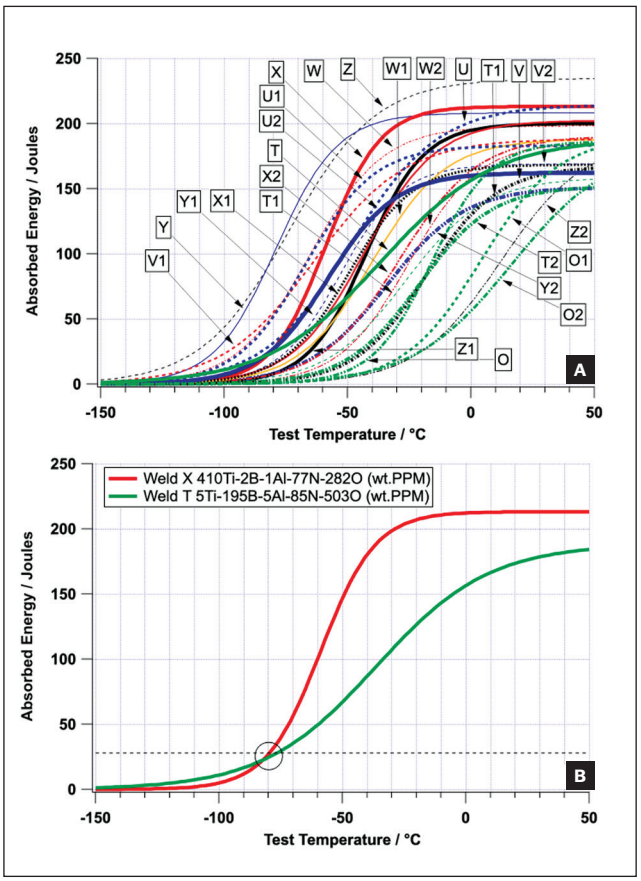

Fig. 1 — A — Charpy energy absorbed vs. temperature curves for all 24 weld metal test samples with varying Ti-Al-B-N combinations. These curves are fitted using the sigmoidal function to the raw data provided by Evans (Ref. 4); B — two of the data corresponding to welds X and T are extracted and replotted to show the limitation of using a singular value of temperature for assessing toughness behavior.

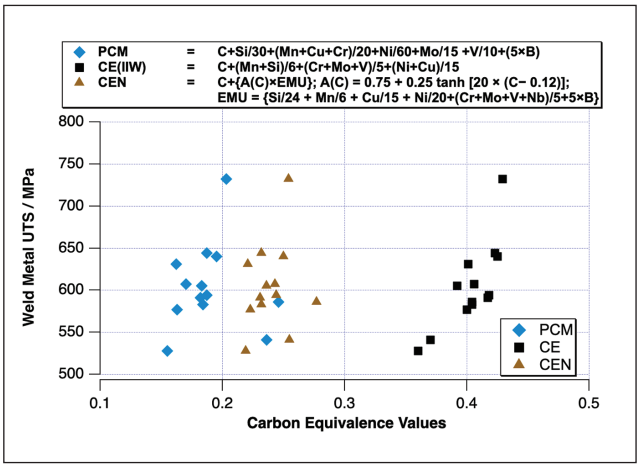

Fig. 2 — Correlation of carbon equivalence values based on various formula with ultimate tensile strength (UTS).

the sub-set) shows a large difference in overall toughness response with temperature, yet both yield a similar 28J transition temperature (Fig. 1B). The predictive power of the numerical models, including the neural net predictors, may well be limited without the inclusion of such critical data.

Carbon equivalence (CE) formulae and strength: The first approach to strength prediction involved three (Pcm, CE_{IIW}, and CEN) constitutive carbon equivalence (CE) equations, each incorporating around nine alloying elements (Fig. 2). It is noteworthy that these equations, outlined in Reference 2, ignore the effect of microalloying additions, except for the inclusion of B for Pcm and CEN. Yet, the authors indicated a limited correlation between ultimate tensile strength (UTS) and the three carbon equivalents. A modest lateral correlation within a single CE group is apparent only for CE_{IIW} that does not include a microalloy component. Thus, it logically follows that the reported CEs are not the cause of the profound variations encountered in microstructure and mechanical properties. The marked difference evident in UTS in the vertical direction is due to a progressive increase in micro-alloying content and its role in controlling the final microstructure. As a result, one can observe the lowest UTS for the weld with no microalloying additions and the highest UTS for the weld with high Si content and an excessive amount of aluminum.

Austenite to ferrite transformation start temperature (T_S) on cooling: In the next step, data was further filtered for compositions representing low N. A linear correlation presents with increasing UTS as transformation start temperature declines was shown with only 6 of the original 24 data points (Fig. 3A). When replotted with all the transformation start data from original reference (Ref. 7) (Fig. 3B), there is no apparent correlation between UTS and transformation start. A different pattern emerges with two regimes. In the first regime, the two points at transformation temperature below 720°C exhibit the active influence of boron, at a low nitrogen concentration of less than 100 wt. ppm. Secondly, marked by the filled symbols, the transformation starts to decrease with higher (> 100 wt. ppm) nitrogen concentration. Interestingly, (Fig. 3C) the calculated transformation-start temperatures (A_{R3}) show no correlation with UTS and no influence of boron. Concerning T_S, the evidence for the present micro-alloyed weldments shows that it remains invariable, except when boron is active. The microalloy-free weld exhibited no acicular ferrite in the top bead whereas the introduction of 30 ppm titanium led to the formation of acicular ferrite, approximately 70% of the constituent (Ref. 8). This variation occurred without any detectable change in either T_S or the UTS, but the Charpy-V curve still was displaced by 50°C, to a lower temperature (i.e., confirmation of the better toughness even in multipass welds due to the addition of microalloying elements). For C-Mn deposits containing microalloying elements, the influence of T_S is of less consequence than the microstructural evolution that subsequently follows. The initial step is for the primary ferrite to delineate the prior austenite grain boundaries followed by the formation of intragranular constituents, depending on the presence or absence of efficacious non-metallic inclusions.

The final mechanical properties, including yield strength, tensile strength, elongation, reduction in area, and Charpy energy transition curves (at 28J and 100J energy levels) are

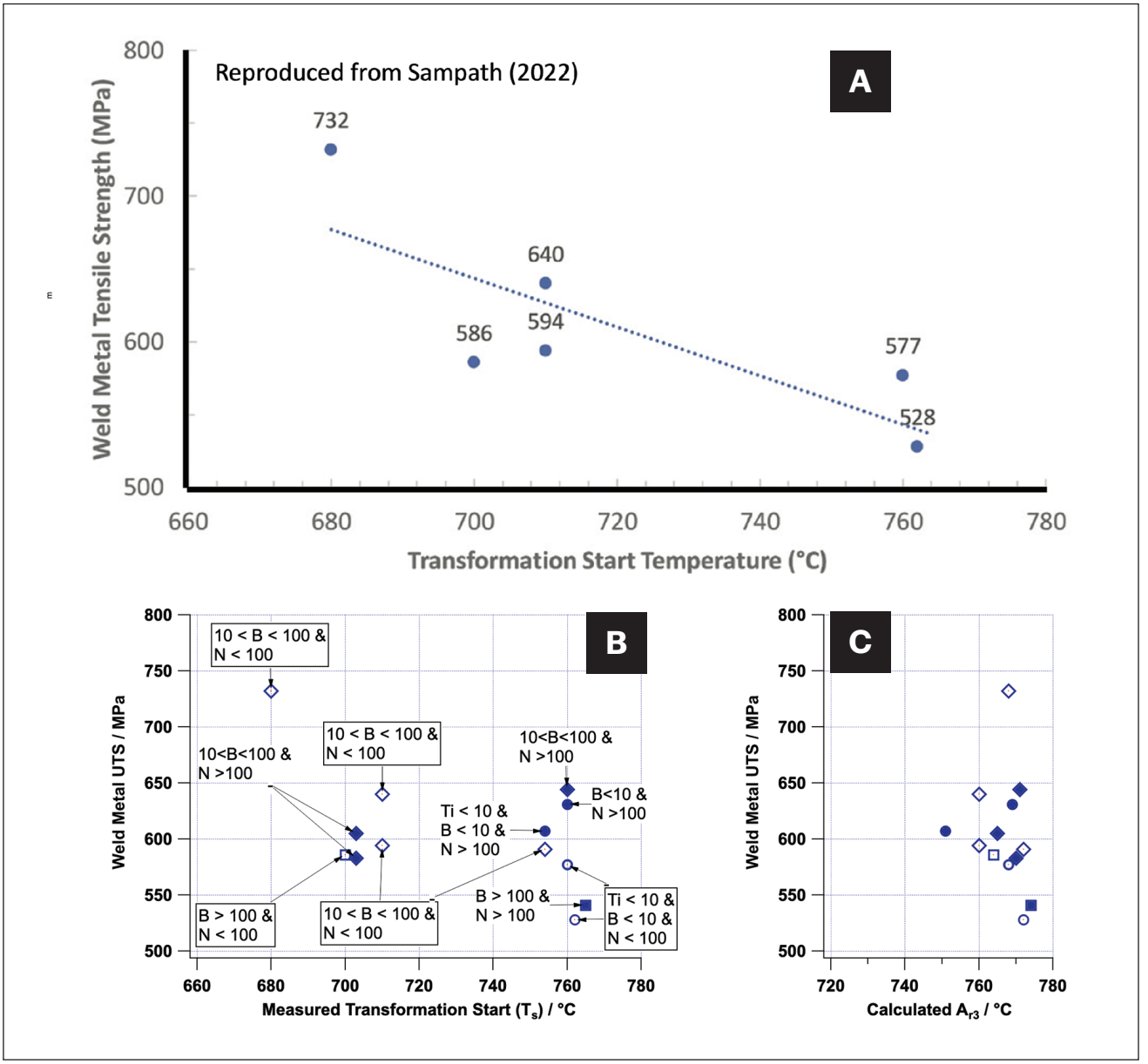

Fig. 3 — A — Published image showing the perceived good correlation between transformation start, A_{r3}, on ultimate tensile strength (reproduced from Ref. 2) for a given cooling rate; B — the same plot with additional data from original Ref. 7; C — correlation of calculated A_{r3} using the data from Ref. 2.

dependent on whether the elements interact or are retained in solution and in turn affect the local microstructures, particularly in the case of nitrogen which can partially be in the free form or in the form of carbides.

This reanalysis reconfirms that the physical metallurgy of ferritic weld metal is complex. Extensive systematic studies over the years (Ref. 8) demonstrated that the final microstructure and properties are controlled by the presence and interactions among sixteen elements (C, Mn, Si, S, P, Al, B, Ti, Nb, V, Ni, Cr, Mo, Cu, O, and N). It is also important to note that the current welds are indeed sub-set (i.e., low hydrogen shielded metal arc welds with deliberate variation in only five elements) of the large scope of welding consumable composition and processing parameters reported in the literature. In contrast, classic carbon equivalence formulae were developed decades ago to assist the industry in mitigating the risk of hydrogen-assisted cracking and embrittlement in various forms with reference to heat-affected zones in base metals (Refs. 9, 10). As such, the number of critical chemical constituents is smaller and does not include the microalloying elements of interest here.

Prediction of mechanical properties with models only sensitive to weld composition: Further correlations were developed using a JWES neural network program (Ref. 5). However, the neural net is limited to the prediction of the temperature to achieve an absorbed energy of 28 J. This coincides with the bottom shelf regimen, where weld deposits having a high Charpy-V upper shelf intersect with those

Table 1 — Historical Ti-B-Al-O-N Weld Metal Compositions

ID	C†	Mn†	Si†	P†	S†	Nb*	B*	Al*	N*	O*	V*	Ti*
O	0.074	1.40	0.25	0.007	0.008	5	1	6	79	475	5	1
W	0.077	1.46	0.27	0.007	0.008	5	3	5	81	459	5	28
X	0.069	1.47	0.45	0.006	0.005	5	2	1	77	282	5	410
Y	0.070	1.57	0.45	0.010	0.006	5	39	13	83	308	5	390
Z	0.072	1.56	0.49	0.010	0.007	5	48	160	67	438	5	420
T	0.064	1.49	0.40	0.005	0.007	5	195	5	85	503	5	5
U	0.073	1.52	0.40	0.011	0.006	5	158	5	84	290	5	390
V	0.078	1.44	0.60	0.007	0.006	5	56	580	41	440	5	540
O1	0.074	1.58	0.28	0.008	0.008	5	5	5	145	404	5	5
W1	0.068	1.40	0.28	0.008	0.010	5	5	5	148	409	5	31
X1	0.066	1.48	0.47	0.011	0.007	5	2	5	164	285	5	410
Y1	0.069	1.48	0.34	0.010	0.007	5	40	5	149	281	5	370
Z1	0.070	1.45	0.43	0.010	0.006	5	37	170	130	439	5	470
T1	0.070	1.55	0.39	0.007	0.007	5	160	6	144	396	5	7
U1	0.066	1.39	0.35	0.009	0.006	5	158	5	138	290	5	360
V1	0.067	1.44	0.63	0.010	0.005	5	44	560	120	473	5	480
O2	0.073	1.66	0.27	0.008	0.009	5	5	5	235	399	5	5
W2	0.069	1.45	0.26	0.009	0.010	5	5	2	226	391	5	29
X2	0.068	1.46	0.47	0.006	0.007	5	2	5	249	297	5	450
Y2	0.069	1.51	0.36	0.008	0.007	5	44	5	232	292	5	410
Z2	0.068	1.45	0.50	0.011	0.006	5	45	180	230	440	5	470
T2	0.064	1.43	0.36	0.008	0.008	5	160	5	233	426	5	5
U2	0.066	1.40	0.36	0.012	0.007	5	167	5	217	297	5	390
V2	0.069	1.42	0.60	0.012	0.006	5	35	560	235	470	5	430

***Limited set of compositions that were used to derive correlations in the literature are highlighted in bold fonts (Ref. 4). †concentrations are given in wt-%; *concentrations are in wt. ppm; concentrations of other elements, such as Cr, Ni, Cu, and Mo, were maintained at the trace levels, i.e., 0.03, 0.03, 0.03, and 0.005 wt-%, respectively. Vanadium concentration was maintained at 5 wt. ppm levels for all welds.**

having a flatter more horizontal profile, as shown in Fig. 1B. The neural network is based on the very same database being used to develop design rules. Further, other aspects have a large impact on weld metal properties, which are not explicitly taken into consideration in the numerical models. For example, the role of free nitrogen that is dissolved either in the ferrite (BCC) structure at low temperature or in the austenite (FCC) structure at high temperature may pose complex microstructure evolution and properties. If the nitrogen precipitates out as carbonitrides in the ferrite, they may function as stress raisers. If they precipitate out in the austenite, they may limit the austenite grain growth and reduce the hardenability. Furthermore, the reheating effects in the multipass welds may also induce tempering that may lead to a reduction in strength and increase in ductility, thereby increasing toughness. The optical observation of acicular ferrite microstructure in the primary weld metal region may not always guarantee good toughness in the Charpy-V-notch samples extracted from multipass regions due to the complex morphology of microconstituents in between the ferrite grains.

Conclusions

1. The carbon equivalent number, derived from classical formulae, has no benefit for the design and optimization of micro-alloyed weld properties because only one of the necessary interactive elements is ever included.

2. Further, knowledge of the temperature for the commencement of the phase change from austenite to ferrite (T_s) is of limited benefit since the microstructural development on subsequent cooling is critically dependent on ppm level changes in the degree of micro-alloying.

3. Since the WJES predictive neural program provides only a temperature to achieve 28 J, corresponding to the lower shelf, it offers little as a suitable design tool, due to the tendency for Charpy-V curves to intersect at low energy values.

4. The use of sequential spreadsheet correlations can be useful in guiding welding electrode design. However, the use of such correlations in predicting actual behavior will be limited when the underlying data is insufficient in breadth and/or depth to resolve interactions among the key input variables (i.e., the five microalloying elements, in this case).

5. Further, the temptation to use multiple sequential data filters to eliminate noise variables and reveal correlations may lead to oversimplification and bias if not adequately moderated by an understanding of the underlying metallurgical and welding engineering principles and critical questioning of underlying assumptions.

Acknowledgment

The contributions of Sudarsanam Suresh Babu related to weld metal microstructure and properties were funded by the Department of the Navy, Office of Naval Research under ONR award number N00014-18-1-2794. Any opinions, findings, conclusions, or recommendations expressed in this material are those of the author(s) and do not necessarily reflect the views of the Office of Naval Research.

References

1. Sampath, K. 2021. Analysis of a high-strength steel SMAW database. *Welding Journal* 100(10): 410-s to 420-s.

2. Sampath, K. 2022. Metallurgical design rules for high strength steel weld metals. *Welding Journal* 101(5): 123-s to 143-s.

3. Varadarajan, R., and Sampath, K. 2023. Application of machine learning to regression analysis of a large SMA weld metal database. *Welding Journal* 102(3): 31-s to 52-s.

4. Evans, G. M. 2015. Database-weld metal composition and properties. DOI: 10.13140/RG.2.1.3628.1764

5. Online calculator for the Charpy impact transition temperature that satisfies the 28J. *www-it.jwes.or.jp/weld_simulator/en/calc6.jsp.*

6. Fujii, H., and Ichikawa, K. 2000. Estimation of weld properties by bayesian neural network. *Welding in the World* 70: 335–339.

7. Ilman, M. N., Cochrane, R. C., and Evans, G. M., 2014. Effect of titanium and nitrogen on the transformation characteristics of acicular ferrite in reheated C-Mn weld metals. *Welding in the World* 58: 1–10.

8. Evans, G. M., and Bailey, N. 1999. *Metallurgy of basic weld metal*. Abington Publishing.

9. Kasuya, T., and Yurioka, N. 1993. Carbon equivalent and multiplying factor for hardenability of steel. *Welding Journal* 72(6): 263-s to 268-s.

10. Yurioka, N., Okumura, M., Kasuya, T., and Cotton, H. J. U. 1987. Prediction of HAZ hardness of transformable steels. *Metal Construction* 19: 217R–223R.

GLYN EVANS is a consultant from Liverpool, UK. **MARIE QUINTANA** is formerly from Lincoln Electric Company, Cleveland, Ohio. **SUDARSANAM SURESH BABU** is the UT-ORNL Governors Chair from the Department of Mechanical, Aerospace, and Biomedical Engineering, The University of Tennessee, Knoxville, Tenn.